Magnetic Resonance Velocimetry in Hydrogen Combustion Chambers – An Initial Comparison with CFD

Swantje Romig[1], Nina Paulitsch[2], Fabrice Giuliani[3], Sven Grundmann[4], Robert Krewinkel[5], Martin Bruschewski[6]

[1, 4, 6] Lehrstuhl Strömungsmechanik, Universität Rostock, Albert-Einstein-Str. 2, 18059 Rostock, Deutschland, vorname.nachname@uni-rostock.de, lsm.uni-rostock.de

[2, 5] Institut für thermische Turbomaschinen und Maschinendynamik, Technische Universität Graz, Inffeldgasse 25 a, 8010 Graz, Österreich, vorname.nachname@tugraz.at

[3] Combustion Bay One e.U. advanced combustion management, Schuetzenhofgasse 22/7, 8010 Graz, Österreich, Fabrice.Giuliani@CBOne.at

Abstract: The mixing process of air and hydrogen as a fuel for combustion is still difficult to model in computational fluid dynamics (CFD) simulations. In this study, a validation data set measured using Magnetic Resonance Imaging (MRI) methods is provided. The measurements were conducted in a water channel experiment. Although slightly varying operating conditions were simulated and measured, it can be concluded that water channel experiments using MRI methods can provide valuable information on the mixing processes that can help during the design of hydrogen burners.

Keywords: Hydrogen, Magnetic Resonance Velocimetry, Turbulent Mixing, Water Channel Experiments, CFD

1 Introduction

Decarbonizing the industry requires several different technologies, and especially in aviation, but also for power supply, combustion of alternative carbon-free fuels like hydrogen plays a role. Hydrogen shows a different behavior from conventional fossil fuels during combustion: It has a higher flame speed, flame temperature, and diffusivity, leading to several challenges like flame stability and NO_x emissions [1], [2]. A crucial aspect here is the turbulent mixing process of the fuel and the air.

Therefore, new burner geometries are developed that are more suitable for hydrogen combustion. During the design process, CFD is a widespread tool. But as the air and hydrogen flows are turbulent and scale-resolving simulations are computationally too expensive, turbulence models are used. For different flows, different turbulence models can be most suitable. Additionally, combustion models are not yet calibrated for hydrogen. Consequently, experimental validation data is useful.

MRI methods, especially Magnetic Resonance Velocimetry (MRV), have already been used to validate other industrial flows like cooling flows [3], [4]. MRV is a noninvasive measurement technique that allows the acquisition of 3D datasets in complex geometries without optical access or seeding that other fluid mechanics measurements would require [5].

MRV can conducted using a conventional clinical MRI scanner. Therefore, water is used as a working fluid because the scanner is tuned to the resonance frequency of protons in water molecules of the human body. To ensure comparability of the measurements in a water channel experiment using MRV with simulation data at real operating conditions, similarity conditions have to be considered. In fluid mechanics, this is typically the Reynolds number, representing the ratio between the inertial and the viscous forces. This is used to scale the air flow and make it comparable to the water flow in the MRV experiment. Compressibility effects of gas flows become relevant above Mach numbers of around 0.3, so these effects can be neglected here. To account for the different densities of air and hydrogen, another scaling is needed. Here, the momentum flux ratio is used, which connects the squared velocities and the densities of both fluids. This way of scaling has already been used in other water channel experiments that investigate the mixing behavior of hydrogen and air [6], [7]. There are two ways to implement this momentum flux ratio scaling. In [7], Sangl et al. modified the hole injection geometry of the hydrogen, while in [6], Jaeschke et al. used the unchanged geometry and modified the flow rates. Jaeschke et al. found some contradictions between the water channel experiments to examine the mixing and the atmospheric test rig experiments to record emissions, but could not identify which experiment caused them. Sangl et al. used the water channel data to calculate NO_x emissions, and also found some deviations from combustion experiments that they assigned to the varying momentum flux ratio due to manufacturing difficulties. In this study, as a first try, the geometry is not modified like in the study of Jaeaschke et al.

Currently, mixing is challenging to capture precisely in an experiment. Especially, as this complex process depends on many factors: the velocity difference between the two flows, the initial level of turbulence, and the turbulence produced by the shear layer. In a swirling flow, the swirl may also contribute to the mixing. Nonetheless, insights into the turbulent mixing process are valuable for combustor design, as they influence flame stability and NO_x emission [2]. However, combustion experiments in realistic operating conditions are extremely expensive, and a limited amount of hydrogen is available. Therefore, preliminary experiments are essential.

The scope of this study is to compare datasets from a CFD simulation to MRV data and evaluate whether MRV data can be used for validation purposes in the design process of hydrogen combustion chambers. Special attention is paid to the injection pattern to assess whether the momentum flux ratio is a useful and sensible similarity condition. The geometry of a burner designed for hydrogen combustion was used [8], [9]. The mean velocity field, turbulence kinetic energy (TKE) as turbulence statistics, and mean concentration of a contrast agent added to the hydrogen stream are measured using MRI methods and compared to RANS simulation data.

2 Methods

2.1 The burner geometry

The premixed swirl stabilized burner geometry that was investigated in this study is further described in [8] and [9]. It is depicted in Figure 1 (a). The air (indicated by red arrows) enters the burner from the left side through a pipe, which is followed by a swirler. The hydrogen is

injected from the injector (black) indicated by blue arrows. It is also swirled and then exits through 11 holes. The premixing zone is followed by a sudden expansion, where combustion should take place. For the CFD, the original scale and size were used, whereas for the measurements, the model was scaled up for a better relative resolution (Figure 1 (b)). The simulation and the measurements were not performed at the exact same operating point, but at comparable conditions. Consequently, this study should be understood as a qualitative comparison with the character of a feasibility study.

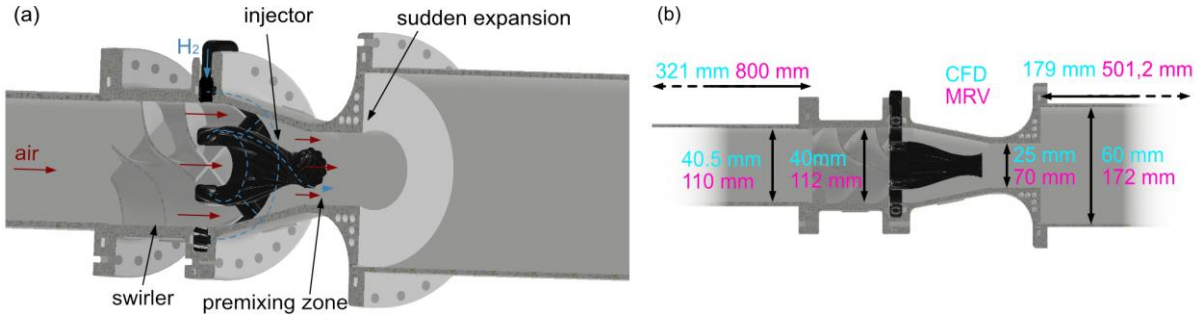

Figure 1: Investigated burner geometry (a) and dimensions (b) for CFD (blue) and MRV (pink)

2.2 CFD

The simulations were performed using OpenFoam 2.4.0 as a RANS (Reynolds-averaged Navier–Stokes) solver. RANS simplifies turbulent fluid flow by averaging the Navier–Stokes equations over time, which reduces the effects of turbulence into modeled terms. This approach makes simulations much less computationally expensive while still providing useful predictions for many engineering flows. The turbulence model used was the realizable k-ϵ model. To model combustion, the flamelet approach was used. To avoid the necessity of solving chemical mechanisms during the simulation, it uses pre-tabulated 1D flamelets to describe local chemistry, temperature, and combustion reactions. The local mixture and the distortion and stretching of the flame by the turbulent flow field are described by means of the mixture fraction, its variance, and the scalar dissipation rate [10]. This means that the mixture ignites automatically where the mixture fraction and scalar dissipation rate lie within a burning flamelet. In this case, it results in a partially attached flame, whereby the velocity field downstream of the injector depends on the flame velocity.

Boundary and shear layers are challenging to predict for this kind of simulation, and the chemical processes are modeled in a simplified way. Thus, the simulation results must be interpreted carefully.

The operating point for the CFD simulation was $\phi = 0.334$, $\dot{m}_{air} = 4.3\ g/s$ and $P = 5\ kW$.

2.3 MRV

The mockup for the MR-investigations was manufactured from PMMA and PA, and acrylic resin via additive manufacturing (SLS and SLA), which are MR-compatible plastics that have a susceptibility similar to water. The susceptibility is a material property that describes the magnetization of a material in a strong magnetic field. If materials have different susceptibilities, this leads to magnetic field distortions affecting the image. The air flow was scaled using the Reynolds number as the similarity condition to account for the change of

working fluid from air to water. Taking measurable velocities, the geometrical limitations of the scanner, relative resolution of the injection holes, and conventional sizes for PMMA pipes into account, a geometrical scaling factor of 2.8 from the original burner size was chosen for the mockup. The dimensions are shown in Figure 1 (b). The flow loop is shown in Figure 2. The red lines indicated the hoses and pipes feeding the air (here modeled by purified water). The pipes upstream of the model are 5 m long with a diameter of 40 mm and are used for the flow to settle. The water is pumped from a 600 l tank with 1 g/l added copper sulfate to enhance magnetic relaxation properties and has a negligible effect on the fluid properties. The water is kept at 20 °C, and the flow rate is 73.8 l/min, resulting in a bulk velocity of the “air” in the premixing zone of 0.32 m/s. The water modeling the hydrogen (blue lines) is pumped either from the same tank for mean velocity and TKE measurements (b) or from an extra tank for concentration measurements (a). The flow rate is 2.33 l/min, and the bulk velocity at the injection holes is 0.34 m/s. This operating point corresponds to an equivalence ratio of $\phi = 0.3$, $u_{air} = 11.9\ m/s$ and $P = 7kW$ from [8]. The equivalence ratio describes the fuel-to-air ratio divided by the fuel-to-air ratio for stochiometric combustion.

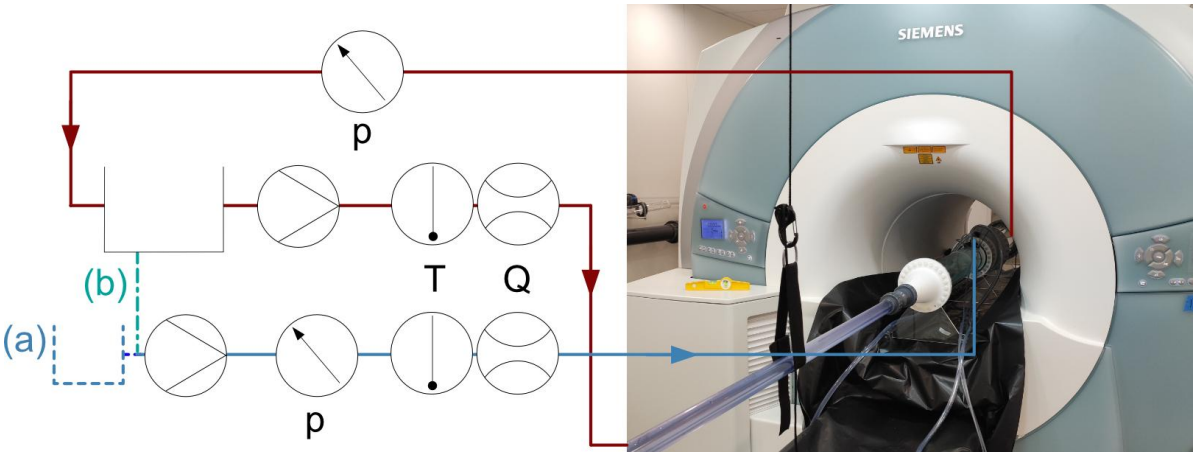

Figure 2: Schematic view of the experimental setup, red: “air” flow loop, blue: “hydrogen” flow loop, (a) setup for concentration measurements, (b) setup for velocity, TKE, and concentration measurements

To obtain a complete dataset for evaluating the turbulent mixing process in this burner mockup, various flow parameters were measured. The mean velocity was measured using the phase contrast MRI method. This principle is described by [5] and [4]. The underlying principle of velocity-sensitive measurements is the encoding of the velocity into the signal’s phase. The same approach is used to quantify turbulence using the intravoxel phase dispersion (IVPD) method. In turbulent flows, fluid particles inside the imaging volume have different velocities. During a velocity-sensitive measurement, they will consequently have different phases. This phase dispersion leads to a signal decay that is related to the amount of turbulence of the flow. The measurement principle is described by [11]. For the TKE measurement, the ICOSA6 encoding scheme with one velocity-compensated and six velocity-sensitive measurements in different directions was employed to measure the full covariance matrix of the velocity and derive the TKE as its trace. Additionally, four different velocity sensitivities (M_1) were used to cover the full dynamic range of the flow. For more details about the measurement technique and data reconstruction, refer to [12] and [13].

To analyze the mixing process, Magnetic Resonance Concentration (MRC) measurements were performed. This method is described by [14] and [15]. The signal magnitude is linearly

dependent on the amount of a contrast agent added to the “hydrogen” flow. In this case, copper sulfate was used. First, calibration scans are done to find the linear range, which is bounded by the reference concentration, here 1 g/l, with a maximum deviation from linearity of 6 % at low concentrations. Then, copper sulfate was only added to the “hydrogen” flow, while purified water was used for the “air” flow for the final concentration measurements. These scans are called standard scans. To account for background effects and provide proper scaling, so-called background and reference scans are needed. For the background scans, both air and hydrogen are represented by purified water, while for the reference scans, both flows are purified water with 1 g/l copper sulfate added. Finally, the concentration of the contrast agent can be calculated by subtracting the background scan’s magnitude from both the standard and the reference scan’s magnitudes and then dividing the former difference by the latter.

For all three measured parameters, a custom gradient echo sequence was used. An echo asymmetry of 0.2 and inverted readout gradients were used to minimize systematic errors [13]. The measurement parameters are summarized in Table 1.

Parameter	Mean velocity	TKE	Concentration
FOV [mm³]	384 x 192 x192	384 x 192 x192	384 x 192 x192
Resolution [mm³]	1 x 1 x 1	1.5 x 1.5 x 1.5	1.5 x 1.5 x 1.5
TE [ms]	2.02	2.94 … 3.81	1.56
TR [ms]	4	4.46 … 5.33	8
Flip angle [°]	15	15	35
# of averages	13 (1 flow off [5])	8	5
M_1 [mT·ms²/m]	10	30, 40, 50, 60	0.11
Measurement time	4h 55 min	9 h	4 h 22 min

Table 1: Mesurement parameters for MRI

The measured flow parameters constitute a complete data set that can be used to investigate turbulent mixing. The concentration field gives an overview of the mixing quality, while the mean velocity and the TKE can be used to examine the relevant underlying mechanisms.

3 Results and Discussion

There are various reasons for differences between the experimental and numerical data, which are briefly introduced at the beginning of this section. The simulation considered the combustion that led to an attached flame at the injector’s tip, influencing the velocity field, while no combustion could be modeled in the water channel experiment. Comparable, but different operating conditions were examined, where the equivalence ratio was very similar, but the velocities were different. While the water-channel experiments were conducted at a distinct operating point with respect to similarity scaling, the corresponding full-scale (air) velocities associated with this operating point are higher than those of the CFD case. The physical velocities in the water channel itself remain lower due to the use of dynamic similarity. Simulations and experiments were also done using different design stages of the combustor, where the premixing zone’s conical and cylindrical areas vary. Finally, the nature

of water channel experiments is a setup with constant density, whereas hydrogen and air have significantly different densities. To account for this, the momentum flux ratio scaling was used, leading to different velocity ratios between the hydrogen and the air in the experiment and the simulation.

Due to these differences between the experimental and the numerical setup, the following comparison is presented on a qualitative level. Using dimensionless parameters, it is estimated whether the flow conditions are comparable such that they produce the same flow phenomena.

Figure 3 shows an overview of the bulk velocity in the z-direction in two planes. It is normalized to the bulk velocity in the premixing zone just upstream of the sudden expansion. The bulk velocities were 0.35 m/s for MRV and 18.55 m/s for the CFD data. The velocity field shows some common features, especially in the top row. The cone appears slightly more open in the CFD case (right), which might be attributed to the higher diffusivity of the hydrogen that cannot be reproduced by water. An obvious difference in the velocity field can be seen in the bottom row. As the experiment used the momentum flux ratio for scaling, the velocity of the “hydrogen” is in the same order as the velocity of the “air”, whereas in the simulation, the hydrogen has about three times higher velocity than the air. This difference was expected and accepted because the mixing behavior was the focus of this study. The measurement uncertainty for the MRV data is 0.019 m/s and was calculated using the difference approach [16].

As this burner geometry uses swirl to stabilize the flame, the swirl number S was calculated for both MRV and CFD. It is used to classify if a central recirculation zone will form and is defined as the ratio of the tangential momentum flux to the axial momentum flux [17]:

$$S = \frac{\int_0^R \rho u_{ax}\, u_{tan} r^2\, dr}{R \int_0^R \rho u_{ax}^2\, r\, dr}, \tag{1}$$

where R is the radius of the premixing zone, ρ is the density, u_{ax} is the axial velocity and u_{tan} is the tangential velocity.

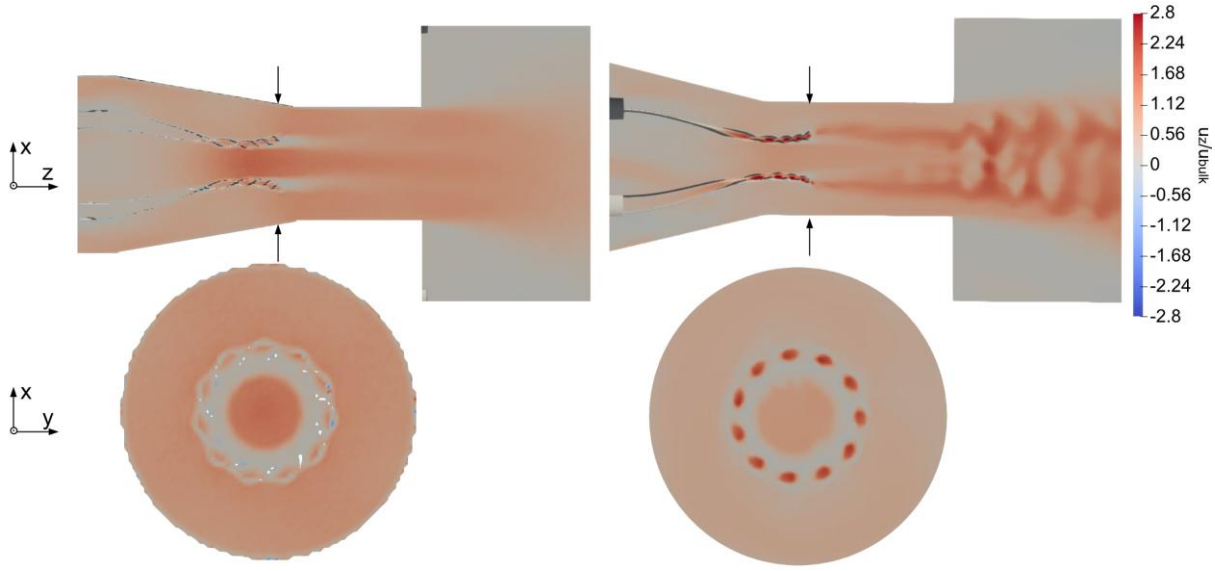

Figure 3: Normalized streamwise velocities for MRV (left) and CFD (right)

The swirl number at the beginning of the premixing zone is about 0.3 for both MRV and CFD. It decreases to about 0.15 for the CFD case and remains constant for the MRV case. Interestingly, S rises to about 0.5 behind the sudden expansion for the MRV data, but remains at about 0.15 for the CFD data. Overall $S < 0.6$ indicates that no central recirculation zone forms, and both flows are comparable in the way that the same jet-like flow phenomena occur, as opposed to a jet centrifuged toward the wall for $S > 0.6$.

The Reynolds number, which was also used for similarity scaling, was 22,368 for the MRV case and 12,012 for the CFD case for the air at the beginning of the premixing zone. Both indicate a turbulent flow, and the mean flow topology, like recirculation zones, is not influenced by this change.

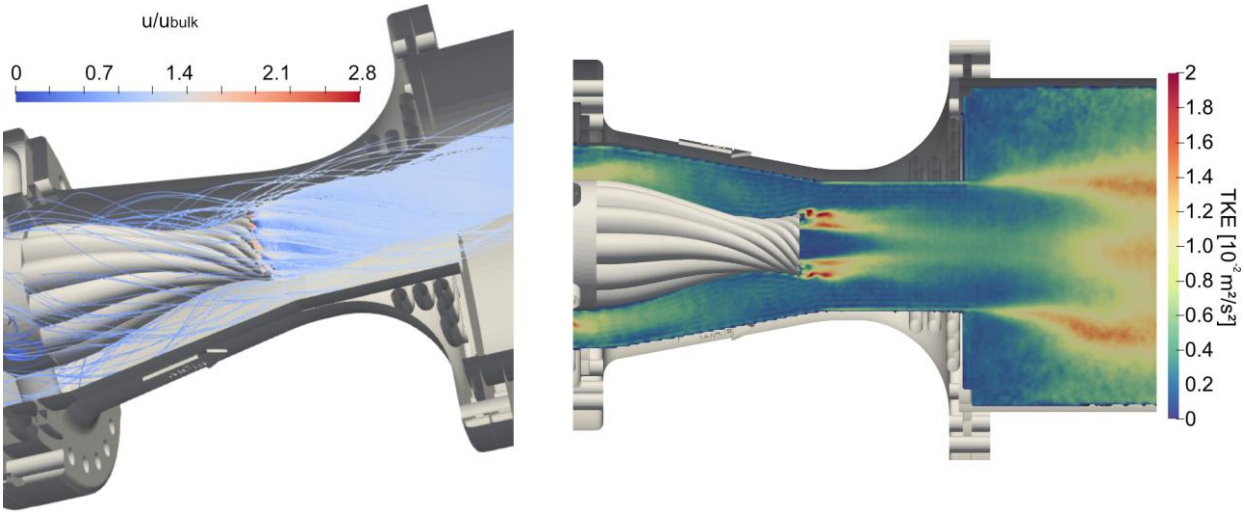

Figure 4: Streamlines from MRV data (left), TKE from MRV data (right)

In Figure 4 on the left side, the streamlines obtained from the MRV data are shown. They show the weak swirl of the flow and give an intuitive overview of the flow field.

The right side of Figure 4 shows the TKE measured using MRV. Turbulence is mainly produced in the shear layer between the injected “hydrogen” and the “air” and at the sudden expansion. This will probably lead to fast mixing of hydrogen and air, which is beneficial and the design goal of the burner. The uncertainty for the TKE determined using the difference approach [16] is 0.0015m²/s².

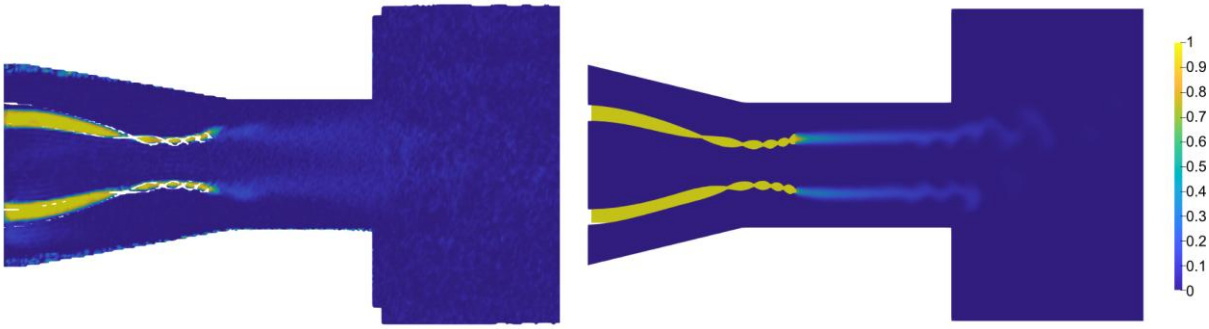

Figure 5: Concentration of contrast agent in MRC (left) and of H_2 in CDF (right)

Figure 5 depicts the concentrations of the contrast agent for MRV on the left side and for hydrogen for CFD on the right side. In both cases, a quick decay in concentration, indicating good mixing, can be observed. In the experiment, the mixing is even faster than in the simulation. The MRC data has a measurement uncertainty of 1.7 %. Due to the modeled combustion in the simulation, which cannot be captured by the water channel experiment, faster mixing would be expected in the simulation. Possible reasons for the opposite outcome could be different initial levels of turbulence due to different Reynolds numbers for MRV and CFD, the different velocity gradients between the air and the hydrogen flow for simulation and experiment, and uncertainties in the computation of shear layers of the RANS model. Nonetheless, the fuel placement is similar for both experiment and simulation.

4 Conclusion

Despite some limitations of this study due to different operating conditions and geometry variations between the simulations and experiments, it showed the potential of water channel experiments using MRI methods scaled via Reynolds number and momentum flux ratio to provide comprehensive datasets for evaluating the turbulent mixing process in hydrogen combustion. The simulation and experiments showed similar flow and mixing patterns, making MRV and MRC valuable tools for insights into the 3D flow field as well as mixing processes and fuel placement.

5 Acknowledgement

This work was funded by the German Federal Ministry for Economic Affairs and Energy under grant number 20E2229 on the basis of the decision by the German Bundestag.

Funded by the Deutsche Forschungsgemeinschaft (DFG, German Research Foundation) - INST 264/222-1.

6 References

[1] Beita, Jadeed, et al. "Thermoacoustic instability considerations for high hydrogen combustion in lean premixed gas turbine combustors: a review." Hydrogen 2.1 (2021): 33-57.

[2] Singh, Gaurav, et al. "A review of hydrogen micromix combustion technologies for gas turbine applications." International Journal of Hydrogen Energy 127 (2025): 295-310.

[3] Siekman, Mike, et al. "A Combined CFD/MRV study of flow through a pin bank." Turbo Expo: Power for Land, Sea, and Air. Vol. 45714. American Society of Mechanical Engineers, 2014.

[4] John, Kristine, et al. "Volumetric Measurements of Mean Velocity Vector and Reynolds Stress Tensor for CFD Validation: Magnetic Resonance Velocimetry in a Nuclear Fuel Assembly Model with Mixing Grids." Flow, Turbulence and Combustion 115.1 (2025): 221-241.

[5] Elkins, Christopher J., and Marcus T. Alley. "Magnetic resonance velocimetry: applications of magnetic resonance imaging in the measurement of fluid motion." Experiments in Fluids 43.6 (2007): 823-858.

[6] Jaeschke, Alexander, et al. "Experimental investigation of a multi tube burner for premixed hydrogen and natural gas low emission combustion." Journal of Engineering for Gas Turbines and Power 145.12 (2023): 121010.

[7] Sangl, J., C. Mayer, and Thomas Sattelmayer. "Prediction of the NO x-Emissions of a Swirl Burner in Partially and Fully Premixed Mode on the Basis of Water Channel LIF and PIV

Measurements." Turbo Expo: Power for Land, Sea, and Air. Vol. 55119. American Society of Mechanical Engineers, 2013.

[8] Paulitsch, Nina, Fabrice Giuliani, and Andrea Hofer. "Validation of a combined optic-acoustic probe on hydrogen flames using an atmospheric lean premix pilot burner." 2023 Symposium on Thermoacoustics in Combustion: SoTiC 2023. 2023.

[9] Paulitsch, Nina, et al. "Progress on the Complete and low-NOx combustion of eco-fuels using a thermo-acoustically-driven, hydrogen-powered pilot stage." Turbo Expo: Power for Land, Sea, and Air. Vol. 86946. American Society of Mechanical Engineers, 2023.

[10] Müller, Hagen, Federica Ferraro, and Michael Pfitzner. "Implementation of a Steady Laminar Flamelet Model for non-premixed combustion in LES and RANS simulations." 8th International OpenFOAM Workshop. 2013.

[11] Dyverfeldt, Petter, et al. "On MRI turbulence quantification." Magnetic resonance imaging 27.7 (2009): 913-922.

[12] Schmidt, Simon, et al. "Reynolds stress tensor measurements using magnetic resonance velocimetry: expansion of the dynamic measurement range and analysis of systematic measurement errors." Experiments in Fluids 62.6 (2021): 121.

[13] Romig, Swantje, et al. "Improving MRI turbulence quantification by addressing the measurement errors caused by the derivatives of the turbulent velocity field–Sequence development and in-vitro validation." Magnetic Resonance Imaging 117 (2025): 110333.

[14] Benson, Michael J., et al. "Three-dimensional concentration field measurements in a mixing layer using magnetic resonance imaging." Experiments in Fluids 49.1 (2010): 43-55.

[15] Banko, Andrew J., et al. "An improved three-dimensional concentration measurement technique using magnetic resonance imaging." Experiments in Fluids 61.2 (2020): 53.

[16] Bruschewski, Martin, et al. "Estimation of the measurement uncertainty in magnetic resonance velocimetry based on statistical models." Experiments in Fluids 57.5 (2016): 83.

[17] Syred, Nicholas, and János M. Beér. "Combustion in swirling flows: a review." Combustion and flame 23.2 (1974): 143-201.